



Detection of fluorine labeled Herceptin using cellular ^{19}F MRI *ex vivo*

Dorota Bartusik^{a,*}, Boguslaw Tomanek^{a,b,c,d}

^a National Research Council Canada, Institute for Biodiagnostics (West), 3330 Hospital Drive NW, Calgary, Alberta T2N 4N1, Canada

^b Cross Cancer Institute, Department of Medical Physics, 11560 University Ave, Edmonton, Alberta T6G 1Z2, Canada

^c Institute of Nuclear Physics, Polish Academy of Sciences, Radzikowskiego 152, 31-342 Krakow, Poland

^d University of Alberta, Department of Oncology, 11560 University Ave, Edmonton, Alberta T6G 1Z2, Canada

ARTICLE INFO

Article history:

Received 14 June 2009

Received in revised form 6 October 2009

Accepted 6 October 2009

Available online 14 October 2009

Keywords:

Drug efficacy

^{19}F MRI

Breast cancer cells

ABSTRACT

The aim of this study was to assess the Herceptin efficacy in *ex vivo* cultures of MCF-7 breast carcinoma cells. Herceptin was used with perfluorooctyl bromide (PFOB) and conjugated with Lipoplex, containing plasmid DNA and Lipofectamine (LipA), to allow fluorine-19 magnetic resonance imaging (^{19}F MRI) study. Treatments such as Herceptin, Herceptin/PFOB and Herceptin/PFOB/Lipoplex were used for *ex vivo* targeting of MCF-7 cells cultured in three-dimensional (3D) geometry using hollow fiber bioreactor (HFB) device. The viability of MCF-7 cells after 72 h treatments decreased to $54 \pm 2\%$, $50 \pm 3\%$ and $45 \pm 1\%$ for Herceptin, Herceptin/PFOB and Herceptin/PFOB/Lipoplex, respectively. The EC_{50} values were $1000 \mu\text{g/ml}$, $930 \mu\text{g/ml}$ and $730 \mu\text{g/ml}$, respectively. The significant correlation between the treatment concentration and efficacy was observed in MCF-7 cell cultures.

Crown Copyright © 2009 Published by Elsevier B.V. All rights reserved.

1. Introduction

HER-2 receptor is an important pathological target for the treatment of breast cancer tumor [1]. HER-2 is expressed at the cells' surface, which makes it accessible to drug binding, therefore breast cancer drugs efficacy has been tested in several preclinical trials [2]. Herceptin, a monoclonal antibody targeting HER-2, has been used as the first-line treatment for patients with metastatic breast cancer [3]. However, about 70% of patients with HER-2 overexpression do not respond to Herceptin therapy [4]. Therefore, for the study of Herceptin, a simple yet efficient method of verifying drug activity is required. Up to date, proton magnetic resonance imaging (MRI) has been used to detect breast tumor morphology, e.g. size [5]. However, we propose to use fluorine-19 (^{19}F) MRI to detect efficacy of Herceptin conjugated with fluorine emulsion. The utilization of ^{19}F MRI allows the imaging of the fluorine labeled cells without any background since there are no endogenous fluorine atoms present in the body [6]. As ^{19}F magnetic resonance probe we used perfluorooctyl bromide (PFOB). The MCF-7 cell cultures were grown in hollow fiber bioreactor (HFB) in 3D cellular geometry resembling *in vivo* cell condition and produce high density cell culture suitable for MRI study. In the previous study we developed 3D MCF-7 and Human T-Lymphoblastoid cells' cultures for the evaluation of cells' oximetry using ^{19}F MRI during treatment with δ -tocopherol [7].

2. Experimental

2.1. Reagents

For targeting HER-2 we used Herceptin (Genentech Inc., San Francisco, CA). All compounds for the cell culture were supplied by Fisher Scientific (Oakland, ON). Trypan blue was supplied by Sigma–Aldrich (Oakville, ON). Lipoplex containing Lipofectamine (LipA) and plasmid DNA were from (Innovita Inc., Geithesburg, MD). Perfluorooctyl bromide (PFOB) was from (SynQest Laboratories Inc., Alauca, FL).

2.2. Cell cultures

2.2.1. Human adenocarcinoma MCF-7 cells

Human MCF-7 cell line was obtained from the American Type Culture Collection (Manassas, VA). HER-2 overexpression of these cell lines was confirmed with cytometric analysis [8]. CO_2 independent medium supplemented with 10% buffered Fetal Bovine Serum (FBS), 1% L-glutamate, and 1% antibiotic (penicillin/streptomycin) was used. Prior to maintenance in HFB, the passaged cells were resuspended in CO_2 independent medium and plated (25 ml , $1 \times 10^6 \text{ cells/ml}$) on a 6-well tissue culture polystyrene (TCPS) plates. Each well was then filled with 2 ml of the CO_2 independent medium and cultured at 37°C under atmospheric CO_2 for 24 h. The cells were maintained in tissue culture flasks and were cultured as monolayer until the number of cells reached $0.5 \times 10^5 \text{ cells/ml}$. 3D cell cultures were grown for 4 weeks. MCF-7 cells were counted at each time point, namely each day.

* Corresponding author. Tel.: +1 403 221 3221; fax: +1 403 221 3230.

E-mail address: dorota.bartusik@gmail.com (D. Bartusik).

2.2.2. Human mammary epithelial cells (HMEC)

HMEC cells (GIBCO Invitrogen, Rockville, MD) were isolated from mammary tissue and cultured in culture flask until the number of cells reached 0.5×10^5 cells/ml. The Medium 171 supplemented with 0.4% bovine extract, 5 mg/l bovine insulin, 0.5 mg/l hydrocortisone and 3 μ g/l human epidermal growth factor were used.

2.2.3. 3D cultures of MCF-7 and HMEC

MCF-7 cells and HMEC cells were seeded in the HFB device (FiberCell Systems Inc., Frederick, MD). The HFB is a closed loop system that consists of porous hydrophilic hollow fiber with 0.1 μ m size pores in polysulfone tubing. For the study we used one fiber in each HFB cartridge. The cell growth medium was fed from a reservoir. We used collagen solution to create an extracellular matrix (ECM) between the cells and the fiber. The polysulfone fiber was coated with protein by flushing with 10 ml of coating solution containing 1 mg collagen per 1 ml Phosphate Buffered Saline (PBS). After the inoculation, the HFB was perfused using a peristaltic pump. The flow of medium started at the rate of 5 ml/min and was gradually increased to 14 ml/min. The pH was measured in the space of HFB device throughout the duration of experiments and was between 6.8 and 7.0. The pH of the cell growth medium was monitored using a pH meter, and the measurements were taken every 24 h for the next 4 weeks. The perfusion medium was changed weekly when the glucose level reached 2 g/l measured with glucometer. The breast cancer cells were allowed to grow in the HFB until the density of the cells reached 10^9 cells/ml.

The number of cells was determined using Trypan blue exclusion method [9]. Briefly, MCF-7 cells and HMEC cells were harvested from HFB device, seeded in 6-well microplates and exposed to 0.4% (w/v) Trypan blue dye solution. Number of cells in the HFB device was determined manually with a hemacytometer chamber (Hausser Scientific, Horsham, PA).

2.3. Treatment with Herceptin

10 ml of Herceptin at concentrations of 0.05 μ g/ml (**H1**), 0.5 μ g/ml (**H2**), 50 μ g/ml (**H3**), 100 μ g/ml (**H4**), 200 μ g/ml (**H5**), 500 μ g/ml (**H6**) and 1000 μ g/ml (**H7**) was used to treat 10^9 cells/ml in HFB device ($n = 3$ for each treatment).

2.4. Preparation of Herceptin/PFOB emulsions (**H8–H14**)

Perfluorooctyl bromide (PFOB) and Herceptin were used for the formulation of Herceptin/PFOB emulsions **H8–H14**. The emulsions were composed of 20% (v/v) PFOB, 2% (w/v) safflower oil and 1.7% (w/v) glycerin, with water comprising the balance. Herceptin was added at concentrations of 0.05 μ g/ml (**H8**), 0.5 μ g/ml (**H9**), 50 μ g/ml (**H10**), 100 μ g/ml (**H11**), 200 μ g/ml (**H12**), 500 μ g/ml (**H13**) and 1000 μ g/ml (**H14**) and the compounds were mixed together.

2.5. Preparation of Herceptin/PFOB/Lipoplex emulsions (**H15–H21**)

Lipoplex was formulated from plasmid DNA mixed with Lipofectamine (LipA) at the molar ratio 1/3. LipA was originally composed of polycationic lipid 2,3-dioleoyl-N-[2(sperminecarboxymido)ethyl]N,N-dimethyl-1-propanaminium trifluoroacetate (DOSPA) and neutral lipid dioleoyl phosphatidylethanolamine (DOPE) [10]. To the obtained Herceptin/PFOB emulsions **H8–H14**, Lipoplex was added to establish Herceptin/PFOB/Lipoplex **H15–H21** emulsions. The molar ratio of Herceptin/PFOB to Lipoplex was 1/3.

2.6. Fluorine emulsion characterization

To optimize reaction time during formulation of **H8–H14** and **H15–H21** emulsions, we measured ^{19}F magnetic resonance signals intensity (SI) of PFOB conjugated with Herceptin and compared with pure PFOB signals which occurred at 0 h, 1 h, 24 h, 48 h and 72 h.

All measurements were performed using 21 cm diameter horizontal bore 9.4 Tesla (T) magnet (Magnex, UK) equipped with a TMX MR console (NRC-IBD, Canada). A custom built solenoidal radio-frequency (rf) coil double-tuned to 376 MHz and 400 MHz corresponding to ^{19}F and ^1H Larmor frequency at 9.4 T, respectively, was used. ^{19}F spectra were acquired using a one-pulse sequence (flip angle 60° ; repetition time (TR) = 800 ms; number of average 2; echo time (TE) = 6 ms).

2.7. Treatments with fluorine emulsions

For the treatment of 10^9 MCF-7 cells/ml in HFB device ($n = 3$ for each treatment) the total volumes of injected **H8–H14** and **H15–H21** emulsions were 10 ml. The cells were incubated with treatments for 24 h, 48 h and 72 h. The day before **H15–H21** were used, the cells were maintained in serum free media without antibiotics.

To test the toxicity of emulsions on health breast tissue, 10^9 HMEC cells/ml in HFB device ($n = 3$ for each treatment) were treated with 10 ml of **H8–H14** and **H15–H21** for 24 h, 48 h and 72 h.

In order to observe the response of cells to treatments visually, we used an inverted microscope (Micro Cap Version 1.0) with ESPA Systems Co., Ltd software.

The influence of PFOB on cell culture was checked using the culture in the presence of PFOB emulsion during 4 weeks. The concentrations introduced to the culture were 20% (v/v) PFOB, 2% (w/v) safflower oil and 1.7% (w/v) glycerin and in this condition cells were grown. Moreover, cells' samples taken after 72 h of incubation with PFOB emulsion prepared without Herceptin as well as **H14** and **H21** emulsions, were lysed with 5 mM Tris-HCl (pH 7.4), the membrane fraction was separated from the cytoplasmic fraction by high-speed centrifugation, and the possible PFOB content in the two fractions was measured using MRI procedure. Moreover, ^{19}F MRS of culture cells treated with **H8–H14** was performed using single pulse measurements (flip angle 60° ; TR = 800 ms; number of average 2; TE = 6 ms).

2.8. MRI measurements

Before treatments ^1H MR images of MCF-7 and HMEC cells were performed using spin echo imaging sequence with TR = 1000 ms, TE = 40 ms, 0.5 mm slice thickness, 2 cm \times 2 cm field of view, 256 \times 256 matrix size and 10 signal averages. After treatments ^{19}F MR images were acquired using a spin echo imaging sequence with TR = 500 ms, TE = 18 ms, 2 cm \times 2 cm field of view, 256 \times 256 matrix size and 10 signal averages. ^1H and ^{19}F MRI were processed with MAREVISI (NRC-IBD, Canada) post-processing software. The acquisition time was 2560 s for ^1H and 1280 s for ^{19}F imaging.

The minimum measurable amount of cells was calculated on the basis of ^{19}F SI measurements using tubes filled with 100, 1000, 10 000, 100 000, 1 000 000, 10 000 000, 100 000 000 and 1 000 000 000 MCF-7 cells and treated with **H8–H21**.

The optimization assays with the dose of emulsion and time of treatment are presented in Table 1. The ^{19}F SI result was used to estimate the number of treated cells. Moreover, the viability data was used to show the number of treated cells. In this case the assay of viable cells before treatment minus the number of viable cells after treatment gave the number of treated cells, respectively, for **H8–H21**.

Table 1
Numbers of unviable MCF-7 cells assayed after treatment with different emulsions H8–H21.

Time	Starting cell numbers	Assay	H8	H9	H10	H11	H12	H13	H14	H15	H16	H17	H18	H19	H20	H21
24 h	100	A	20 ± 2	21 ± 3	29 ± 5	30 ± 1	33 ± 3	35 ± 3	38 ± 4	26 ± 3	29 ± 2	31 ± 2	36 ± 5	38 ± 4	33 ± 1	39 ± 9
24 h	100	B	11 ± 3%	22 ± 3%	31 ± 4%	39 ± 5%	49 ± 2%	70 ± 3%	82 ± 1%	15 ± 1%	20 ± 2%	32 ± 5%	39 ± 1%	49 ± 1%	69 ± 2%	77 ± 13%
24 h	10	A	2.4 ± 0.3	2.6 ± 0.8	2.8 ± 0.6	2.8 ± 0.5	3.1 ± 0.2	3.4 ± 0.4	3.7 ± 0.2	2.0 ± 0.5	2.0 ± 0.5	2.9 ± 0.2	3.2 ± 0.3	3.3 ± 0.3	3.0 ± 0.2	3.8 ± 0.3
24 h	10	B	9 ± 2%	23 ± 3%	32 ± 2%	38 ± 2%	46 ± 3%	68 ± 3%	82 ± 3%	12 ± 3%	19 ± 1%	30 ± 4%	40 ± 3%	42 ± 1%	72 ± 3%	80 ± 3%
24 h	1	A	0.24 ± 0.08	0.24 ± 0.07	0.27 ± 0.07	0.27 ± 0.03	0.30 ± 0.02	0.32 ± 0.04	0.36 ± 0.01	0.20 ± 0.07	0.2 ± 0.02	0.28 ± 0.01	0.32 ± 0.07	0.31 ± 0.01	0.29 ± 0.01	0.39 ± 0.02
24 h	1	B	8 ± 0.9%	25 ± 3%	33 ± 3%	34 ± 2%	45 ± 1%	67 ± 2%	83 ± 2%	13 ± 4%	21 ± 3%	30 ± 3%	35 ± 3%	47 ± 4%	71 ± 2%	78 ± 2%
24 h	0.1	A	0.022 ± 0.005	0.023 ± 0.005	0.026 ± 0.008	0.03 ± 0.007	0.028 ± 0.007	0.03 ± 0.002	0.03 ± 0.008	0.02 ± 0.009	0.02 ± 0.001	0.027 ± 0.002	0.03 ± 0.003	0.03 ± 0.002	0.02 ± 0.002	0.039 ± 0.007
24 h	0.1	B	10 ± 3%	21 ± 1%	30 ± 2%	29 ± 4%	47 ± 2%	65 ± 2%	79 ± 3%	10 ± 2%	20 ± 2%	31 ± 1%	36 ± 2%	48 ± 3%	68 ± 4%	77 ± 2%
48 h	100	A	26 ± 3	27 ± 5	30 ± 5	32 ± 1	33 ± 3	35 ± 3	39 ± 6	26 ± 7	29 ± 8	31 ± 2	39 ± 2	43 ± 2	41 ± 9	47 ± 2
48 h	100	B	10 ± 2%	23 ± 2%	32 ± 2%	40 ± 4%	50 ± 5%	72 ± 4%	87 ± 4%	11 ± 4%	22 ± 3%	34 ± 2%	35 ± 4%	51 ± 5%	71 ± 2%	78 ± 2%
48 h	10	A	2.6 ± 0.8	2.5 ± 0.6	2.9 ± 0.4	3.0 ± 0.9	3.2 ± 0.4	3.2 ± 0.5	3.8 ± 0.7	2.0 ± 0.5	2.8 ± 0.7	30 ± 3	2 ± 0.3	4.0 ± 0.3	4.1 ± 0.3	4.5 ± 0.3
48 h	10	B	9 ± 3%	22 ± 1%	33 ± 4%	41 ± 2%	48 ± 4%	70 ± 2%	81 ± 3%	9 ± 3%	23 ± 3%	31 ± 1%	33 ± 2.3%	52 ± 3%	72 ± 2%	70 ± 3%
48 h	1	A	0.25 ± 0.02	0.25 ± 0.09	0.29 ± 0.01	0.28 ± 0.05	0.30 ± 0.05	0.32 ± 0.07	0.38 ± 0.02	0.20 ± 0.04	0.27 ± 0.03	3.0 ± 0.3	0.2 ± 0.03	3.8 ± 0.1	4.0 ± 0.3	4.4 ± 0.3
48 h	1	B	8 ± 1%	21 ± 1%	34 ± 3%	43 ± 3%	49 ± 2%	73 ± 2%	80 ± 3%	9 ± 2%	22 ± 2%	30 ± 2%	36 ± 4%	53 ± 2%	73 ± 4%	69 ± 2%
48 h	0.1	A	0.023 ± 0.002	0.023 ± 0.006	0.027 ± 0.009	0.027 ± 0.008	0.028 ± 0.004	0.033 ± 0.001	0.037 ± 0.008	0.2 ± 0.3	0.026 ± 0.002	0.028 ± 0.003	0.02 ± 0.003	0.035 ± 0.003	0.037 ± 0.003	0.047 ± 0.002
48 h	0.1	B	10 ± 2.3%	22 ± 2%	32 ± 3%	44 ± 2%	47 ± 3%	68 ± 1%	80 ± 4%	8 ± 4%	25 ± 1.3%	32 ± 2%	40 ± 2%	52 ± 1%	72 ± 3%	10 ± 1.3%
72 h	100	A	27 ± 1	28 ± 6	31 ± 4	33 ± 1	30 ± 6	37 ± 2	43 ± 9	27 ± 2	30 ± 9	31 ± 3	38 ± 3	42 ± 1	41 ± 4	51 ± 4
72 h	100	B	12 ± 1%	20 ± 2%	32 ± 2%	43 ± 2%	52 ± 4%	72 ± 1%	87 ± 5%	13 ± 0.5%	24 ± 1%	31 ± 3%	41 ± 3%	53 ± 3%	73 ± 2%	80 ± 1%
72 h	10	A	2.7 ± 0.8	2.7 ± 0.4	3.0 ± 0.7	3.2 ± 0.3	3.4 ± 0.4	3.5 ± 0.8	4.2 ± 0.5	2.6 ± 0.1	2.7 ± 0.1	3.1 ± 0.3	3.2 ± 0.2	4.0 ± 0.2	3.8 ± 0.4	4.8 ± 0.5
72 h	10	B	11 ± 1%	22 ± 2%	34 ± 3%	44 ± 5%	51 ± 1%	73 ± 4%	81 ± 2%	11 ± 2%	23 ± 2%	30 ± 2.3%	42 ± 2%	55 ± 4%	75 ± 4%	79 ± 2%
72 h	1	A	0.26 ± 0.02	0.24 ± 0.06	0.28 ± 0.06	0.33 ± 0.04	0.35 ± 0.05	0.34 ± 0.05	0.42 ± 0.04	0.25 ± 0.03	0.27 ± 0.03	0.30 ± 0.01	0.30 ± 0.01	0.37 ± 0.4	0.36 ± 0.5	0.47 ± 0.2
72 h	1	B	10 ± 1%	22 ± 1%	35 ± 2%	42 ± 2%	50 ± 3.3%	72 ± 4%	80 ± 2%	10 ± 1%	25 ± 2%	30 ± 2%	45 ± 2%	54 ± 2%	74 ± 2%	82 ± 3%
72 h	0.1	A	0.023 ± 0.003	0.023 ± 0.005	0.026 ± 0.004	0.031 ± 0.007	0.033 ± 0.003	0.033 ± 0.008	0.039 ± 0.002	0.025 ± 0.002	0.027 ± 0.004	0.028 ± 0.004	0.029 ± 0.002	0.036 ± 0.007	0.039 ± 0.007	0.049 ± 0.001
72 h	0.1	B	12 ± 2%	23 ± 1%	35 ± 2%	45 ± 3%	53 ± 1.3%	75 ± 4%	88 ± 7%	9 ± 1%	22 ± 4%	30 ± 2%	47 ± 5%	56 ± 2%	76 ± 2%	83 ± 4%

All cell numbers are $\times 10^7$ cells/ml. Table presents the mean value from 3 assays for each sample.

A, numbers of unviable cells calculated as a starting number of viable cells minus number of viable cells after treatment. Viable cells were determined using Trypan blue assay; B, ^{19}F SI values as compared to pure compounds H8–H21.

10^9 MCF-7 cells/ml in HFB device ($n = 3$ for each treatment) was measured using ^{19}F MRI after 72 h exposure to **H8–H21**. The number of treated cells was estimated using regression data of ^{19}F MRI. The choice of regression equation for these calculations was based on the starting concentration of **H8–H21** used to treatment.

2.9. Calibration curve

The 30 ml of (each emulsion) **H8–H21** were introduced into separate HFB device and MRI scans were performed. ^{19}F SI was measured directly from axial slice of HFB device [11]. The changes in ^{19}F SI at different **H8–H21** concentrations were observed and the calibration curves were prepared, as ^{19}F SI is linearly related with the amount of ^{19}F molecules [12]. The ^{19}F SI of pure PFOB was considered as 100% of SI. Percentage change in ^{19}F SI was normalized to the pure PFOB using the following equation: ^{19}F SI (% change) = $[(U - L)/U] \times 100\%$, where $L = ^{19}\text{F}$ SI of PFOB in emulsions (**H8, H15**), (**H9, H16**), (**H10, H17**), (**H11, H18**), (**H12, H19**), (**H13, H20**) and (**H14, H21**) and U is the ^{19}F SI of pure PFOB.

2.10. Statistical analysis

All results are expressed as a mean \pm SD. The differences between groups at each time point were identified by one-way ANOVA. Statistical comparison between two independent variables was determined by two-way ANOVA with Dunnett's correction. The differences with p -values < 0.05 were considered statistically significant. The data were analyzed using the Sigma Stat Soft (Chicago, IL) software.

3. Results

The numbers of MCF-7 and HMEC cells in the HFB device increased during 4 weeks (Fig. 1). In the HFB culturing device it was possible to determine higher densities of cells close to the fiber possibly due to the influence of medium flow that allowed optimum metabolites and waste concentration.

^1H MR images performed on cultures before treatment showed localization of cells in HFB device. Moreover, ^1H images allowed to monitor changes in the localization of cells, thus providing anatomical information of the cultures and showed 3D cells aggregation in the HFB device (Fig. 2A).

After 24 h of treatment with **H1–H7** the MCF-7 cells viabilities were $80 \pm 1\%$, $77 \pm 4\%$, $74 \pm 2\%$, $70 \pm 3\%$, $66 \pm 4\%$, $63 \pm 3\%$ and $61 \pm 1\%$, respectively. The exposure of MCF-7 cells to **H8–H14** showed the viability equal to $75 \pm 6\%$, $72 \pm 5\%$, $69 \pm 6\%$, $67 \pm 3\%$, $65 \pm 5\%$, $62 \pm 1\%$ and $56 \pm 4\%$, respectively. While using **H15–H21**,

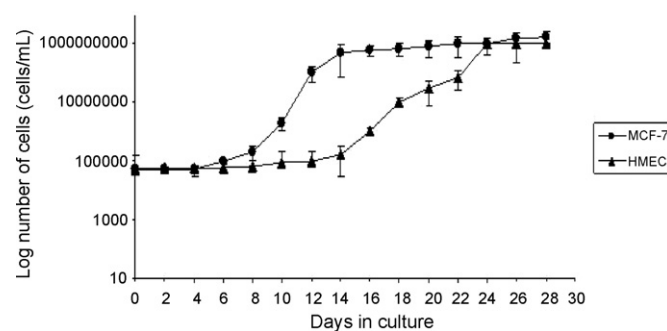


Fig. 1. Cells growth.

the treated cells showed significant decrease and the viability decreased to $74 \pm 4\%$, $70 \pm 4\%$, $67.2 \pm 5\%$, $64 \pm 3\%$, $61 \pm 6\%$, $60 \pm 5\%$ and $59 \pm 4\%$, respectively. The measured R^2 values (Pearson Coefficient of Determination) for viability data after 24 h exposure to drug were 0.9726, 0.8557 and 0.9588 for **H1–H7**, **H8–H14** and **H15–H21**, respectively.

The cells' viabilities treated with **H1–H7** after 48 h were $79 \pm 5\%$, $75 \pm 5\%$, $72 \pm 5\%$, $69 \pm 9\%$, $65 \pm 3\%$, $59 \pm 2\%$ and $58 \pm 4\%$, respectively. After 48 h exposure to **H8–H14**, the viabilities decreased to $79 \pm 5\%$, $78 \pm 3\%$, $75 \pm 2\%$, $70 \pm 4\%$, $68 \pm 4\%$, $61 \pm 4\%$ and $54 \pm 5\%$, respectively. After treatment with **H15–H21**, the percentage of viabilities decreased to $75 \pm 5\%$, $67 \pm 2\%$, $68 \pm 5\%$, $63 \pm 4\%$, $61 \pm 1\%$, $61 \pm 4\%$ and $53 \pm 3\%$, respectively. After 48 h the decreases of viability data-sets were collected with R^2 values 0.9471, 0.8193 and 0.9014 for **H1–H7**, **H8–H14** and **H15–H21**, respectively.

Within 72 h the viabilities decreased to $76 \pm 3\%$, $73 \pm 2\%$, $70 \pm 2\%$, $67 \pm 5\%$, $63 \pm 5\%$, $57 \pm 7\%$ and $54 \pm 2\%$, respectively, for **H1–H7**. After 72 h, the viabilities of MCF-7 were $73 \pm 3\%$, $65 \pm 2\%$, $61 \pm 6\%$, $57 \pm 1\%$, $55 \pm 2\%$, $53 \pm 1\%$ and $50 \pm 3\%$ when treated with **H8–H14**. When **H15–H21** were used, the treated cells showed decreased viabilities equal to $71 \pm 4\%$, $63 \pm 4\%$, $58.2 \pm 5\%$, $57 \pm 1\%$, $55 \pm 2\%$, $52 \pm 3\%$ and $45 \pm 1\%$, respectively. At the same time the viability of control MCF-7 cells was $97 \pm 7\%$, $96 \pm 8\%$ and $95 \pm 7\%$ after 24 h, 48 h and 72 h. After 72 h the viability changes were linear and reached values of R^2 equal to 0.9455, 0.9342 and 0.9374 for **H1–H7**, **H8–H14** and **H15–H21**, respectively.

The HMEC normal cells treated with **H8–H14** did not show decrease in cells' growth for 24 h and 48 h. After 72 h the decreases were equal to $3 \pm 1\%$, $2.7 \pm 1.1\%$, $3.3 \pm 0.9\%$, $3.2 \pm 2\%$, $4 \pm 1\%$, $7 \pm 2\%$ and $7.3 \pm 1.9\%$, respectively. At the same time the decreases of cells viability were $3.2 \pm 0.3\%$, $2.9 \pm 1\%$, $2.3 \pm 1\%$, $3 \pm 1.5\%$, $4 \pm 1.3\%$, $7.2 \pm 2.1\%$ and $7.3 \pm 1.9\%$ for **H15–H21**, respectively. The mean val-

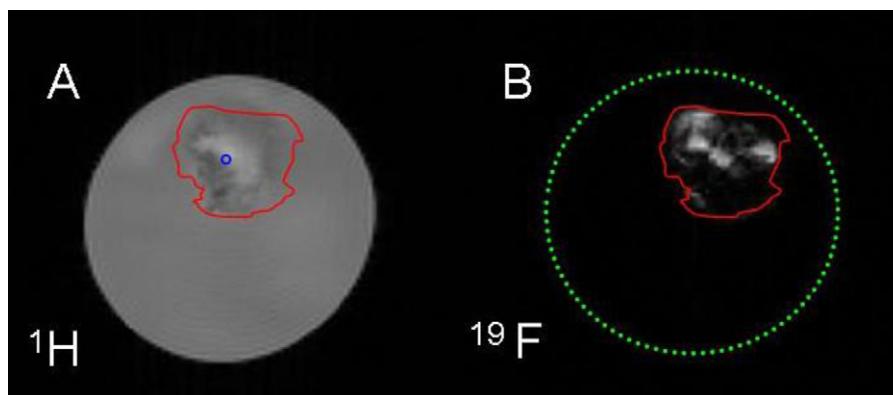


Fig. 2. ^1H image (9.4T) of a single slice showing the cells before treatment (A) and ^{19}F image (9.4T) after 72 h exposure to **H21**. The red lines indicate the region of cells, the green line indicates contour of HFB device and the blue line shows the fiber. (For interpretation of the references to color in this figure legend, the reader is referred to the web version of the article.)

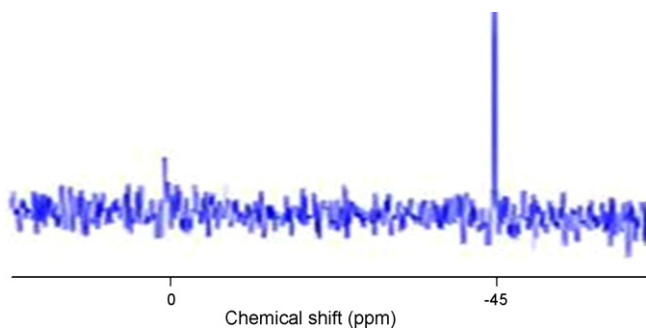


Fig. 3. Example of ^{19}F MRS of cells treated with **H21**. The peak at 0 ppm describes CF_3^- of the reference (pure PFOB) added to cells. The chemical shift value of -45 ppm describes CF_3^- of **H21** after HER-2 targeting. The concentration ratio of PFOB (reference) to PFOB incorporated in **H21** used to treatment was 1:10.

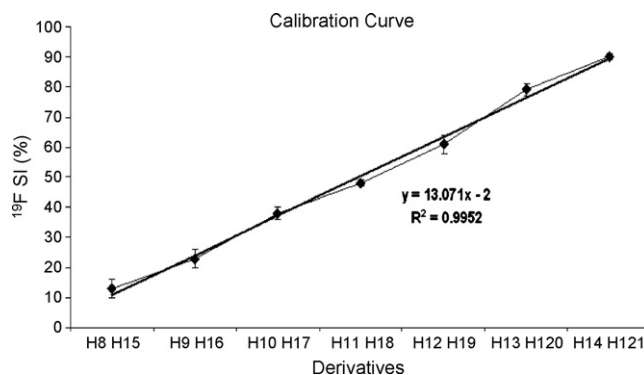


Fig. 4. The calibration curve, where “y” is a unit in (%) and “x” is a unit in ($\mu\text{g}/\text{ml}$).

ues of decreases in viabilities were equal to decreases observed in non-treated cells.

^{19}F MRS signals of pure PFOB were presented at -48 ppm ($\eta\text{-CF}_2$), -40 ppm ($\gamma\text{-}\zeta\text{CF}_2$), -36 ppm ($\beta\text{-CF}_2$), 0 ppm (CF_3) and 18 ppm ($\alpha\text{-CF}_2$) and described according to the nomenclature by Mason and Antich [13]. The peaks of PFOB in **H8–H14** were shifted to -70 ppm ($\eta\text{-CF}_2$), -62 ppm ($\gamma\text{-}\zeta\text{-CF}_2$), -58 ppm ($\beta\text{-CF}_2$), -22 ppm (CF_3) and -4 ppm ($\alpha\text{-CF}_2$). Moreover in **H15–H21**, the peaks were shifted to -75 ppm ($\eta\text{-CF}_2$), -67 ppm ($\gamma\text{-}\zeta\text{-CF}_2$), -63 ppm ($\beta\text{-CF}_2$), -27 ppm (CF_3) and -9 ppm ($\alpha\text{-CF}_2$). In samples of **H8–H14** and **H15–H21** for the calibration 0 ppm (CF_3), pure PFOB was introduced to samples.

Also, PFOB emulsions were detectable by ^{19}F -MRS measurement in the treated cell cultures. In particular, Fig. 3 shows the spectrum of the cells treated with Herceptin/PFOB/Lipoplex **H21** emulsion. As expected, the loss of **H21** signals on ^{19}F MRS was by the targeting of HER-2. Fig. 3 shows the fluorine signal (-45 ppm) in culture cells treated with **H21**. Preferably, the value of chemical shift indicated CF_3^- group of PFOB after treatment of HER-2 with **H21**. The intensities of other signals were too small for detection. One possible explanation is that different magnetic susceptibilities of water and PFOB might lead to distortions of the local magnetic field, thereby causing the MR line shape to broaden.

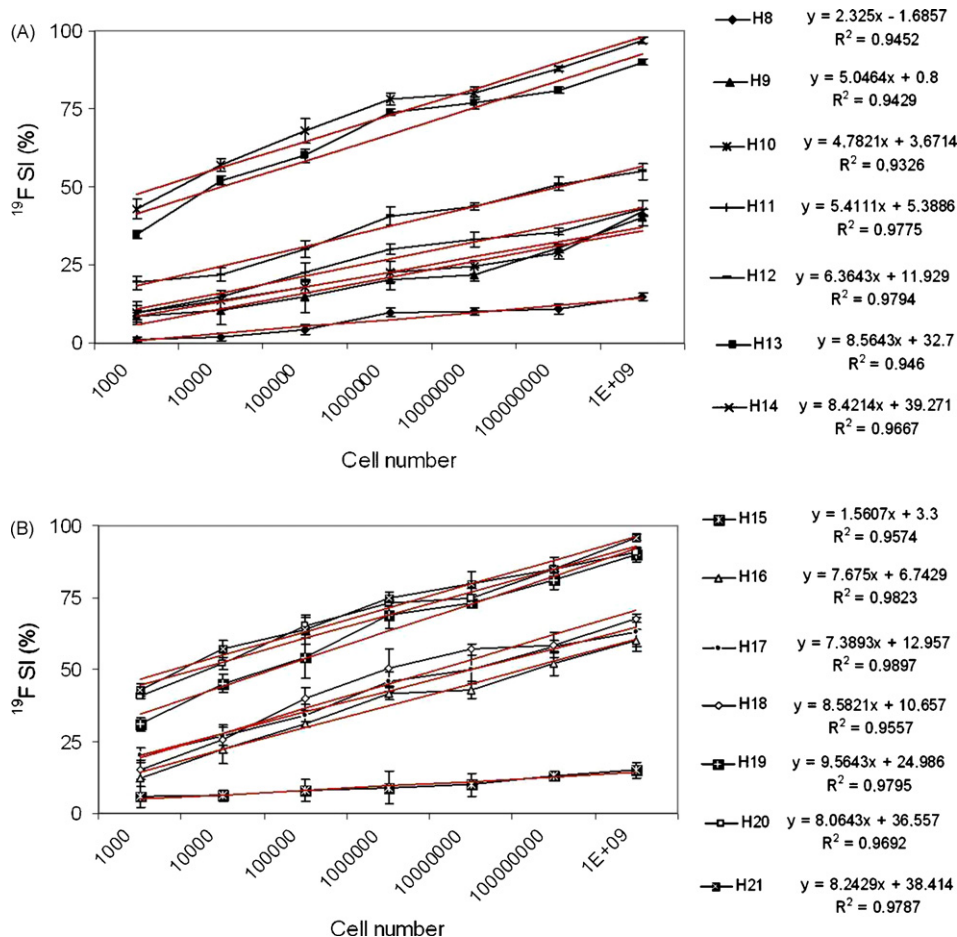


Fig. 5. Number of cells vs. increase of ^{19}F SI for **H7–H14** (A) and **H15–H21** (B). (100% corresponds to SI of pure **H7–H21** without cells).

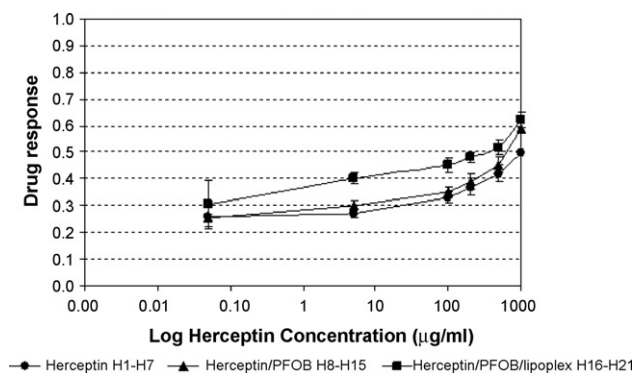


Fig. 6. Efficacy of H1–H21 emulsions in MCF-7 cell cultures.

The absolute number of treated cells was estimated from the ^{19}F MR images using ^{19}F SI of cells which internalize the H8–H14 and H15–H21 emulsions. To quantify the concentrations of ^{19}F , we used the calibration curve $y = 13.071x - 2$ with $R^2 = 0.9952$, where “y” is a unit in (%) and “x” is a unit in ($\mu\text{g/ml}$) (Fig. 4). ^{19}F SI was measured across a slice.

H8–H14 and H15–H21 emulsions incubated with known numbers cells showed that higher doses and longer time of treatment resulted in increased ^{19}F cellular uptake (Fig. 5). The detection limit, due to insufficient ^{19}F signal of targeted cells in HFB device, was 1000 cells while cells were treated using H8–H14 and H15–H21.

The linear functions and regressions described the use of H8–H21 to known numbers of cells (Fig. 5). ^{19}F SI and a number of non-viable cells were 10% higher for cells treated with H15–H21 as compared with cells treated with H8–H14 after 24 h (Table 1). After 48 h the ^{19}F SI of treated cells showed increase in unviable numbers of cells for 6% and 10% while targeted with H8–H14 and H15–H21, respectively. As expected, both values of cells visible with ^{19}F SI increased after 72 h of exposure to emulsions. The observed ^{19}F SI of cells increased by 2% for H8–H14 and H15–H21, as compared with the amount of cells after 48 h treatment. ^{19}F MRI allowed localization of the treated cells in HFB device (Fig. 2B). No ^{19}F signal was observed from extracellular media, for instance compounds that have not been taken up by cells because fresh media were flushed right after treatment. Therefore, ^{19}F SI value is the ^{19}F SI which was measured as a regional signal and then the mean value was calculated.

The used PFOB emulsions allow strong and selective accumulation. Ultimately, the dual use of perfluorocarbon emulsions for both site targeted Herceptin delivery and ^{19}F MR imaging may provide both imaging of cell culture as well as conclusive evidence that Herceptin delivery is localized within the area of interest.

For both types of emulsions, H8–H14 and H15–H21, the increases in emulsion efficacy were observed as compared to Herceptin H1–H7 (Fig. 6). The mean EC_{50} values were 1000 $\mu\text{g/ml}$, 930 $\mu\text{g/ml}$ and 730 $\mu\text{g/ml}$, for H1–H7, H8–H14 and H15–H21, respectively.

The advantage of the used ^{19}F MRI is its selectivity, as only fluorine emulsion labeled cells are visible. The quantifications of cell vitality using Trypan blue showed that viable cells are not affected by ^{19}F emulsions. However, the cells with ^{19}F uptake were visible using ^{19}F MRI and were non-viable using Trypan blue. Both, ^{19}F MRI and Trypan blue assays showed to be a complementary for the viability measurement.

While HMEC were flushed with H8–H14 and H15–H21 emulsions, the cells did not show any ^{19}F MRI signal. After flushing with fresh medium and return to the medium without treatment, the cells grew as before treatment.

The observations of cells under microscope demonstrate that, when viewed under 200 \times magnification, the control MCF-7 and

HMEC cells had a smooth cell wall. The cell wall of Herceptin/PFOB-exposed appeared pulled and shifted. The Herceptin/PFOB/Lipoplex treated cells showed blobbing and demonstrated more extensive cell wall damage.

The cells growing with the presence of PFOB did not show any decreases in growth and the viability was the same to control cells after 4 weeks in culture. However, cells do not spread while using oil emulsion in growth medium. Moreover, the membrane fraction was separated from the cytoplasmic fraction by high-speed centrifugation. In the cytoplasmic fraction was no detectable PFOB and all the PFOB was associated with the membrane fraction.

After 24 h, the quantitative comparison of treated cells showed that H15–H21 were the most effective emulsions. The mean amounts of non-viable cells treated with H8–H14 and H15–H21 detected using ^{19}F SI were $2.3 \pm 0.5 \times 10^8$ and $3.1 \pm 0.7 \times 10^8$, respectively. After 48 h, the treated numbers of cells increased to $3.3 \pm 0.3 \times 10^8$ for H8–H14, $3.7 \pm 0.5 \times 10^8$ for H15–H21, as shown by ^{19}F SI assays. However, the responses of cells to 72 h exposure were $4.0 \pm 0.2 \times 10^8$ non-viable cells for H8–H14 and $4.8 \pm 0.3 \times 10^8$ for H15–H21.

4. Discussion

The application of non-proton MRI to biomarkers monitoring has the advantage over standard proton MRI in cancer research. The lack of background MR signal and selective labeling with ^{19}F , ^{13}C or ^{15}N has resulted in increased applications of heteronuclear MRI. Of particular interest is ^{19}F , whose NMR sensitivity similar to ^1H . Therefore ^{19}F MRI has a potential to provide accurate concentration of markers within a given region of tissue.

In our study, a breast cancer drug, Herceptin, was selected for the ^{19}F MRI *ex vivo*. Due to the ability of labeling Herceptin with PFOB, ^{19}F MRI measurements provide selective information about targeted sites, allowing tracking and showing Herceptin efficacy. While the number of cells possible to target with ^{19}F labeled drug decreased, ^{19}F SI resulted in lower uptake by cells, thus ^{19}F MRI quantified the Herceptin efficacy. Moreover, while the number of viable cells decreased, ^{19}F SI values increased in the region of cells.

To prepare the PFOB emulsions, the fluorochemical liquid and the lipids components were mixed together. It was already known that the liquid PFOB in emulsions is surrounded by a lipid that is functionalized to bind to some therapeutic agents [14]. Therefore Herceptin was covalently coupled to the surface layer of the emulsion. PFOB was as a core and a coating lipid mixture provides a vehicle for Herceptin. Preferably, polar groups such as amine, esters groups as well as relatively hydrophobic alkyl may interact with amide functional groups, primary and secondary amines, carboxylic acid as well as hydrophobic groups in Herceptin through hydrogen bonding and/or hydrophobic interaction. In particular, where a plasmid DNA targeting agent was included, the coating employed a cationic lipid (LipA). Moreover, the non-covalent bonds are critical in targeting processes in which large molecules bind specifically to the receptors.

It has also been postulated that the lipid which coated PFOB is able to couple directly to a targeted receptor or can include intermediate component which is covalently coupled to them [15]. Alternatively, the cell surface receptor can be targeted through a linker, or may contain a non-specific coupling agent such as biotin. Also, the coating may be cationic lipid so that negatively charged targeting agents or can be adsorbed to the surface. A number of observations indicate that the interaction between antibody and targeted receptor is driven by non-specific electrostatic interaction.

As shown, the use of PFOB emulsions requires careful evaluation of their direct effect on cancer cells with other therapeutic agents. Thus, MRI can detect and quantify PFOB emulsions in cancer by

measuring the unique fluorine signal of PFOB. Immediately after the injection of PFOB emulsions, the cells appear brighter due to its PFOB uptake and targeting of receptors by Herceptin. Moreover, PFOB, to be administered in cells, must be dispersed into emulsions which reduce the interracial tension between water and fluorine compounds. Moreover, emulsions facilitated delivery of Herceptin to targeted cells. The use of lipid greatly increases the propensity for hemifusion or enhances contact between the drugs and the targeted cell surface.

In order to simulate *in vivo* conditions with high density of cells for cellular MRI study, we grew the cells in high density and 3D geometry. The 3D cell cultures better capture the real cell–cell and cell–matrix interactions [16]. Moreover, monolayer 2-D cultures fail to obtain some substances, such as albumin and fibroblast [17] which are produced within human organisms and fail to mimic biochemical parameters of tissue [17]. Therefore, the study shows that viability results obtained from 3D cultures are biologically appropriate for drug efficacy study.

Previous studies reported that Herceptin (10–1000 µg/ml) inhibits the growth of breast cancerous cells by 30–50% over 72 h [18]. Currently, among applications of PFOB emulsion, distribution to organs after injection *in vivo*, tumor oxygenation and tissue perfusion, were studied [19,20]. In this study, the potential use of PFOB with Herceptin in emulsions forms were presented. It has already been shown that Lipofectamine (LipA) used *in vitro* transfers the transfected material into the cell through lipid membrane [10]. Therefore, we used cationic lipoplex combined with Herceptin/PFOB emulsion, to assess drug efficiency.

In conclusion ¹⁹F MRI showed cellular accumulation of PFOB due to targeting of HER-2 by Herceptin. We have shown that PFOB emulsions are promising intracellular delivery media for Herceptin.

References

- [1] D. Artemov, N. Mori, R. Ravi, Z.M. Bhujwala, Magnetic resonance molecular imaging of the HER-2/neu receptor, *Cancer Res.* 63 (2003) 2723–2727.
- [2] A. Subramanian, K. Mokbel, The role of Herceptin in early breast cancer, *Int. Semin. Surg. Oncol.* 5 (2008) 9.
- [3] S.C. Wang, L. Zhang, G.N. Hortobagyi, M.C. Hung, Targeting HER-2: recent developments and future directions for breast cancer patients, *Semin. Oncol.* 28 (6 Suppl 18) (2001) 21–29.
- [4] L. Gianni, The “Other” signaling of trastuzumab: antibodies are immunocompetent drugs, *J. Clin. Oncol.* 26 (2008) 1778–1780.
- [5] J.K. Kim, W. Kucharczyk, R.M. Henkelman, Cavernous hemangiomas: dipolar susceptibility artifacts at MR imaging, *Radiology* 187 (1993) 735–741.
- [6] W. Liu, J.A. Frank, Detection and quantification of magnetically labeled cells by cellular MRI, *Eur. J. Radiol.* 70 (2009) 258–264.
- [7] D. Bartusik, B. Tomanek, D. Siluk, R. Kaliszan, G. Fallone, The application of ¹⁹F magnetic resonance *ex vivo* imaging of three-dimensional cultured breast cancer cells to study the effect of δ-tocopherol, *Anal. Biochem.* 387 (2009) 315–317.
- [8] E.T.H. Doeppler, I.K. Yan, S. Goodison, P. Storz, Protein kinase D1 regulates MMP expression and inhibits breast cancer cell invasion, *Breast Cancer Res.* 11 (2009) R13.
- [9] K. Takahashi, G. Loo, Disruption of mitochondria during tocotrienol-induced apoptosis in MDA-MB-231 human breast cancer cells, *Biochem. Pharmacol.* 67 (2004) 315–324.
- [10] J.H. Felgner, R. Kumar, C.N. Sridhar, C.J. Wheeler, Y.J. Tsai, R. Border, P. Ramsey, M. Martin, Enhanced gene delivery and mechanism studies with a novel series of cationic lipid formulations, *J. Biol. Chem.* 269 (4) (1994) 2550–2561.
- [11] M. Srinivas, P.A. Morel, L.A. Ernst, D.H. Laidlaw, E.T. Ahrens, Fluorine-19 MRI for visualization and quantification of cell migration in a diabetes model, *Magn. Reson. Med.* 58 (4) (2007) 725–734.
- [12] L. Li, D.V. Kodibagkar, Y. Jian-Xin, R.P. Mason, ¹⁹F-NMR detection of lacZ gene expression via the enzymic hydrolysis of 2-fluoro-4-nitrophenyl β-D-galactopyranoside *in vivo* in PC3 prostate tumor xenografts in the mouse, *FASEB J.* 21 (2007) 2014–2019.
- [13] R.P. Mason, P.P. Antich, Tumor oxygenation tension: measurement using Oxygent as a ¹⁹F NMR probe at 4.7 T, *Artif. Cells Blood Substit. Immob. Biotechnol.* 22 (1995) 1361–1367.
- [14] A.T. King, B.J. Mulligan, K.C. Lowe, Perfluorochemicals and cell culture, *Bio/Technology* 7 (1989) 1037–1042.
- [15] G.M. Lanza, S.A. Wickline, Targeted ultrasonic contrast agents for molecular imaging and therapy, *Curr. Probl. Cardiol.* 28 (2003) 625–653.
- [16] A. Abbott, Cell culture: Biology’s new dimension, *Nature* 424 (2003) 870–872.
- [17] C. Fischbach, H.J. Kong, S.X. Hsiang, M.B. Evangelista, W. Yuen, D.J. Mooney, Cancer cell angiogenic capability is regulated by 3D culture and integrin engagement, *Proc. Natl. Acad. Sci. U.S.A.* 106 (2) (2009) 399–404.
- [18] P. Kauraniemi, S. Hautaniemi, R. Autio, J. Astola, O. Monni, A. Elkhouloun, A. Kallioniemi, Effects of Herceptin treatment on global gene expression patterns in HER-2 amplified and nonamplified breast cancer cell lines, *Oncogene* 23 (2004) 1010–1013.
- [19] L. Vitu-Loas, C. Thomas, N. Chavaudra, M. Guichard, Radiosensitivity, blood perfusion and tumor oxygenation after perfluorobron emulsion injection, *Radiother. Oncol.* 27 (1993) 149–155.
- [20] A.J. McGoron, R. Pratt, J. Zhang, Y. Shiferaw, S. Thomas, R. Millard, Perfluorocarbon distribution to liver, lung and spleen of emulsions of FTBA in pigs and rats and PFOB in rats and dogs by ¹⁹F NMR Spectroscopy, *Artif. Cells Blood Substit. Immob. Biotechnol.* 22 (1995) 1243–1250.